

Substituent and Solvent Effects on Square-Planar–Tetrahedral Equilibria of Bis[4-(arylimino)pentan-2-onato]nickel(II) and Bis[1-aryl-3-(phenylimino)butan-1-onato]nickel(II) Complexes

Yukie Mori,[1] Hitoshi Shirase,[2] and Yutaka Fukuda*[1]

[1]Department of Chemistry, Faculty of Science, Ochanomizu University, 2-1-1 Otsuka, Bunkyo-ku, Tokyo 112-8610

[2]Nichiyu Giken Kogyo Co., Ltd., 21-2 Matobashinmachi, Kawagoe 350-1107

Received April 7, 2008; E-mail: fukuda.yutaka@ocha.ac.jp

Nickel(II) bis(Schiff base) complexes, NiL_2 (**1a**–**1f**) and NiL'_2 (**2a**–**2e**) (where L = 4-(arylimino)pentan-2-onate and L′ = 1-aryl-3-(phenylimino)butan-1-onate), exist in an equilibrium of square-planar (Sp) and tetrahedral (Td) forms in non-coordinating solvents. The Td form is more stabilized in polar solvents such as CH_2Cl_2 than in non-polar solvents such as toluene. Thermodynamic data were determined from temperature-dependent ^{1}H NMR contact shift. It is suggested for **1a**–**1f** that the oxygen atoms in Td form interact with solvent such as chloroform via hydrogen bonding. With increase in electron-donating ability of the substituents on aryl groups, the Td form becomes more favored. The free energy change roughly correlates with Hammet's σ_p value. The UV–vis–NIR spectra indicated that the ligand field strength increases with the electron-donating ability of the substituents in both the Sp and Td forms. Results of DFT calculation suggest that the observed substituent effect may result from small perturbation of the metal–ligand bonding character.

Some four-coordinated nickel(II) complexes exist in an equilibrium of diamagnetic ($S = 0$) square-planar (Sp) and paramagnetic ($S = 1$) tetrahedral (Td) forms in non-coordinating solvents. The configurational isomerization causes changes in color due to difference in the d–d transition energy. Reversible color change based on the equilibrium shift is one typical example of thermochromism involving inorganic compounds.[1] The Sp–Td conversion is a fast unimolecular process and alters not only color but also magnetic susceptibility and dipole moment of the complex. Such systems may potentially be utilized as temperature sensors or temperature-driven molecular switches. The equilibria of configurational isomers also affect reaction rates of ligand substitution, which may provide fruitful information on reaction mechanisms.[2]

Thermodynamic properties of the Sp–Td equilibria depend on substituents in ligands. For bis(β-ketoimine) complexes **1**, **2**[3] (Chart 1), and bis[(*N*-salicylidene)alkylamine] complexes **3**,[2,4] the position of equilibrium largely depends on steric repulsion between the ligands. Complexes with bulkier ligands favor Td form, since the interligand separation is larger in Td form than in Sp form. On the other hand, only a few studies have been reported for electronic effects of substituents on the equilibrium: Eaton et al. reported correlation of free energy changes (ΔG) with Taft's σ_I values for nickel *N*,*N*′-bis(p-substituted phenyl)aminotroponeiminates **4** (aminotroponeimine = 1-amino-7-imino-1,3,5-cycloheptatriene),[5] while Pignolet et al. reported a linear relationship between ΔG and Hammett's σ_p for bis(p,p′-substituted diphenylmethylphosphine)nickel dihalides **5**.[6]

In the present study, the effects of electronic properties of substituents on the Sp–Td equilibria have been investigated for bis[4-(arylimino)pentan-2-onato]nickel **1a**–**1f** and bis[1-aryl-3-(phenylimino)butan-1-onato]nickel **2a**–**2e** (Chart 2). Interpretation of the observed tendency is discussed with the

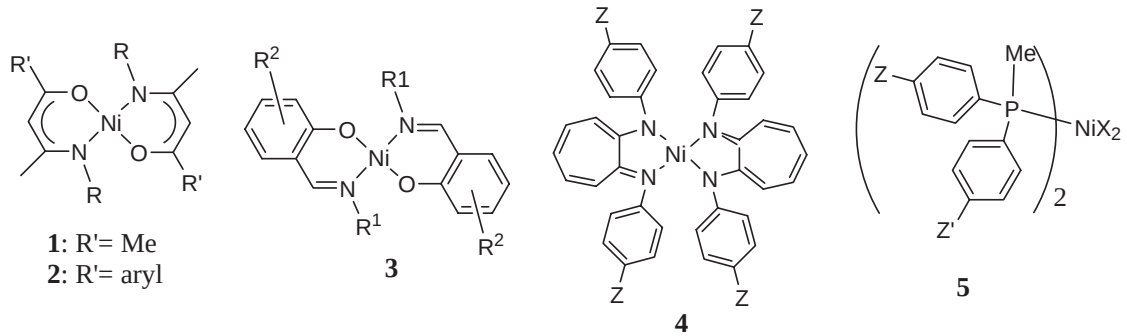

Chart 1.

Published on the web September 11, 2008; doi:10.1246/bcsj.81.1108

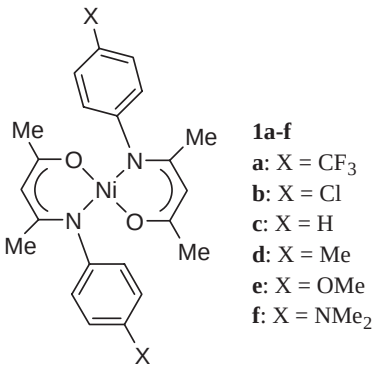

1a-f
a: X = CF_3
b: X = Cl
c: X = H
d: X = Me
e: X = OMe
f: X = NMe_2

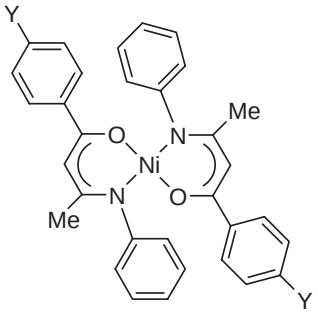

2a, c, d, e
a: Y = CF_3
c: Y = H
d: Y = Me
e: Y = OMe

Chart 2.

help of MO calculations. Solvent effects on the enthalpy changes (ΔH) and entropy changes (ΔS) have also been investigated, which provides information on specific solvation for each form.

Experimental

Materials. All the solvents used for measurements were dried over Molecular Sieves 4A. Pyridine was dried over KOH pellets. Schiff base ligands were synthesized from acetylacetone or (p-substituted) benzoylacetone and (p-substituted) aniline in the presence of montmollironite K-10 (Aldrich) under ultrasound irradiation.[7] The nickel complexes were prepared according to the literature[8] from the ligand and $(Et_4N)_2[NiBr_4]$[9] in *tert*-butyl alcohol distilled from CaH_2. Crude products were recrystallized from benzene–hexane. Complexes **1b**–**1f** and **2c** and **2d** are known compounds.[10] The purity of the complexes was checked with ^{1}H NMR spectroscopy (See Supporting Information).

Bis[4-(4-trifluoromethylphenylimino)pentan-2-onato]nickel (1a). ^{1}H NMR (toluene-d_8, 293 K): δ 7.32 (4H, d, $J = 8$ Hz), 6.67 (4H, d, $J = 8$ Hz), 4.12 (2H, s), 0.95 (6H, s), 0.81 (6H, s). FAB-MS m/z 542 (M^+).

Bis[3-(phenylimino)-1-(4-trifluoromethylphenyl)butan-1-onato]nickel (2a). ^{1}H NMR (toluene-d_8, 323 K): δ 7.83 (4H, br s), 7.28 (4H, d, $J = 8$ Hz), 6.85 (4H, d, $J = 8$ Hz), 6.33 (4H, br d), 5.76 (2H, br t), 0.67 (2H, br s), −0.50 (6H, s). FAB-MS m/z 666 (M^+).

Bis[3-(phenylimino)-1-(4-methoxyphenyl)butan-1-onato]-nickel (2e). ^{1}H NMR (toluene-d_8, 323 K): δ 8.95 (4H, br), 8.04 (4H, d, $J = 8$ Hz), 7.28 (4H, br d), 6.68 (4H, br d), 4.62 (2H, br), 3.33 (6H, s), −2.41 (6H, s), −4.38 (2H, s). FAB-MS m/z 590 (M^+).

Physical Measurements. Mass spectra were obtained on a JEOL JMS-700 Mstation in the fast atom bombardment (FAB) mode using 3-nitrobenzyl alcohol as a matrix. ^{1}H NMR (400 MHz) spectra were recorded on a JEOL JNM-AL400 spectrometer. UV–vis–NIR spectra were obtained on a Shimadzu UV-3600 spectrophotometer.

Formation Constants of Pyridine Bis-Adducts. Formation of bis-pyridine adducts is represented by eq 1.

$$[NiL_2]\ (Td) \underset{K}{\rightleftharpoons} [NiL_2]\ (Sp) \overset{2py}{\underset{K_{py}}{\rightleftharpoons}} [NiL_2(py)_2] \quad (1)$$

Spectrophotometric titration was performed at 300 K. A small aliquot of a toluene solution of pyridine was successively added to a toluene solution (3 mM) of the complex and the UV–vis–NIR spectra were recorded. No intermediate mono-adduct was distinguishably observed in the course of titration. According to Knoch et al.,[4c] interconversion of Sp and Td forms is rapid and the formation constant K_{py} is represented by

$$K_{py} = C_{[NiL_2py_2]}/(C_{[NiL_2]}C_{py}{}^2) \quad (2)$$

where $C_{[NiL_2]}$ is the concentration of four-coordinated complex as a total of Sp and Td forms. The K_{py} value was estimated from the absorbance changes at the characteristic absorption bands of the initial four-coordinated and the final six-coordinated species by the methods in literature.[2]

Equilibrium Constants of Sp–Td Isomerization. Each sample solution (0.4 cm^3) containing 5–10 mM of the complex was placed in a thick-walled NMR tube with a gas-tight Teflon valve. ^{1}H NMR spectra were recorded at various temperatures. Although the complex was gradually hydrolyzed by residual water, the decomposition percentage was less than 5% after the measurements and the chemical shift of each signal was unaffected by the free ligand liberated by hydrolysis. The sample temperature was calibrated using methanol and ethylene glycol.[11] The mole fraction of Td form, x_{Td}, was determined from the chemical shift of β-protons at each temperature. In this type of tetrahedral nickel complexes, pseudo-contact shift was negligibly small compared with the contact shift,[3a] and hence the observed chemical shift can be given by $\delta_{obs} = \Delta\delta_{con} + \delta_{dia}$. The contact shift, $\Delta\delta_{con}$, is given by eq 3:[3,12]

$$\Delta\delta_{con} = -x_{Td}a(\gamma_e/\gamma_H)g\beta S(S+1)/(6SkT) \quad (3)$$

where a is the electron–nuclear hyperfine coupling constant, and the other symbols have their usual meanings. δ_{dia} is the chemical shift of a pure diamagnetic complex. Here, it was assumed that $\delta_{dia} = \delta_{ligand} - 0.2$, where δ_{ligand} is the chemical shift of the free ligand, because it was reported for similar systems that the chemical shifts of the β-protons in Zn^{II} complex shift to higher field by 0.1–0.2 ppm than those in the free ligand.[13] The other parameters used were: $g = 2.3$, $a = 0.825$ G for **1a**–**1f** or 0.855 G for **2a**–**2e**, which were average values reported for closely similar complexes.[3,13] Thus, the equilibrium constant K [$=x_{Td}/(1 - x_{Td})$] was determined from the x_{Td} value and ΔG ($= -RT \ln K$) was calculated at each temperature.

X-ray Crystallography of 1e. Intensity data were collected on a Mac Science M03XHF four-circle diffractometer with graphite-monochromatized Mo Kα radiation ($\lambda = 0.71073$ Å) by ω–2θ scan technique up to $2\theta = 55.0°$ at 298 K. The intensities were corrected for Lorenz and polarization, and absorption correction was made using ψ-scan. 2826 reflections were measured, of which 2631 reflectiones were unique and used for structure determination. The crystal data were: $C_{24}H_{28}N_2NiO_4$, triclinic, $P\bar{1}$, $a = 6.4868(14)$ Å, $b = 8.338(2)$ Å, $c = 11.169(2)$ Å, $\alpha =$

94.32(2)°, $\beta = 104.81(2)°$, $\gamma = 98.56(2)°$, $V = 573.4(2)$ Å^3, $Z = 1$, $D_x = 1.353$ Mg m^{-3}, $\mu = 0.878$ mm^{-1}. The structure was solved by direct method with SIR92[14] and refined by full-matrix least-squares techniques with anisotropic thermal parameters for non-H atoms using SHELXL97.[15] The hydrogen atoms were isotropically refined. The final R and R_w values were 0.034 and 0.095, respectively, and S value was 1.084 using a weighting scheme of $w = 1/[\sigma^2(F_o^2) + (0.0663P)^2 + 0.1062P]$ where $P = (F_o^2 + 2F_c^2)/3$.

Crystallographic data have been deposited with Cambridge Crystallographic Data Centre: Deposition number CCDC-687742. Copies of the data can be obtained free of charge via http://www.cam.ac.uk/conts/retrieving.html (or from the Cambridge Crystallographic Data Centre, 12 Union Road, Cambridge, CB2 1EZ, UK; Fax: +44 1223 336033; e-mail: deposit@ccdc.cam.ac.uk).

DFT Calculations. Structures of Sp and Td forms were optimized with B3LYP/6-31G* level using the Gaussian 03 program package.[16] Complex **1c** (X = H), model **A** (X = F) having electron-withdrawing substituents, and model **B** (X = NH_2) having electron-donating substituents were examined. The initial structure for Sp form was taken from the structure of **1e** determined by X-ray crystallography. Sp form was assumed to be C_i symmetry, while Td form C_2 symmetry. Then, single-point energy calculations were done with slightly different basis sets: 6-31G* for C and H atoms; 6-311+G* for Ni, N, and O atoms; and 6-31G(d′,p′) for F atoms. The computations were performed at the Research Center for Computational Science, Okazaki, Japan.

Results and Discussion

UV–Vis–NIR Spectra. Toluene solutions of **1a–1f** exhibited two absorption bands around 16400 and 20500 cm^{-1} due to d–d transitions of the Sp form. The absorption maxima shifted to higher energy with increase in electron-donating ability of the substituents, indicating that the ligand field is strengthened, as shown in Table 1. Complexes **2a–2e** showed an absorption band around 16000 cm^{-1}, and the band position did not vary with the substituent.

In halogenated hydrocarbon solvents such as $CHCl_3$ and $CHCl_2CHCl_2$, particularly at high temperatures, a weak absorption band was observed in the NIR region. This absorption is assigned to the lowest d–d transition of the Td form.[3] This band also tends to shift to higher energy with increasing electron-donating ability of the substituents.

Table 1. Absorption Maxima of Complexes **1** and **2** in Toluene at Room Temperature

Complex	X or Y	ν_{max}/cm^{-1} (ε/cm^{-1} mol^{-1} dm^3)		
		ν_1 (Sp)	ν_2 (Sp)[a)]	ν_1 (Td)[a),b)]
1a	CF_3	16100 (47)	20300 (82)	
1b	Cl	16300 (51)	20400 (90)	6400
1c	H	16350 (49)	20500 (88)	
1d	CH_3	16400 (52)	20550 (94)	
1e	OCH_3	16500 (57)	20600 (106)	6450
1f	NMe_2	16600 (83)	20700 sh	6480
2a	CF_3	16000 (59)		
2c	H	16000 (62)		
2d	CH_3	16000 (43)		
2e	OCH_3	15900 (59)		

a) Partially overlapped with tail of another absorption band at a higher wavenumber. b) In $CHCl_3$ at 320 K. Very weak absorption band due to a low fraction of Td form in an equilibrium mixture.

Difference in the ligand field strength was reflected in the formation constant of pyridine adduct. On addition of excess pyridine to a toluene solution of **1**, formation of an octahedral bis-adduct was evidenced by the appearance of an absorption band around 10000 cm^{-1} accompanied by disappearance of the absorption bands characteristic of the Sp form. The overall formation constants of pyridine bis-adducts, K_{py} (eq 2), were (449 ± 8) and (8.0 ± 1.0) M^{-2} for **1a** and **1f**, respectively, in toluene at 300 K. It has been reported for salicylaldimine (=salicylideneamine) complexes that the tetrahedrally coordinated complexes form pyridine much less adduct.[4] In the present case, the fraction of Td form is 0.006 for **1a** or 0.057 for **1f** in toluene at 300 K, indicating that the four-coordinate complex exists substantially in Sp form in either case. These results indicate that **1a** with the weaker ligand field accepts two pyridine molecules more readily than **1f**.

Solution Equilibria between Sp and Td Forms. The Sp–Td equilibrium constants were determined from the contact shift of β-protons. Figure 1 shows the temperature dependence of the free energy change for **1a–1f** in toluene-d_8. A linear relationship was observed in the ΔG vs. T plot over a relatively wide range of temperature. Linear temperature dependence was also observed in other non-coordinating solvents such as $CDCl_3$.

The enthalpy and entropy changes are listed in Table 2. The ΔH and ΔS values for **1c** and **1d** in $CDCl_3$ showed relatively good agreement with the corresponding values reported by Everett and Holm,[3a] although they were determined from the contact shift of α-Me protons using an equation slightly different from eq 2. Clear substituent effects can be seen particularly for **1a–1f**: with increase in electron-donating ability of X, ΔH decreases, that is, the Td form becomes more favorable. A similar trend was observed in **2a–2e**, although the effect was smaller. The free energy changes at 298 K, ΔG_{298}, correlate with the Hammett's σ_p value as shown in Figure 2. The entropy change ΔS varies not so much with the substituent for either **1** or **2**. Among bis-chelate Ni^{II} complexes **1–4**, the order of ΔS value in $CDCl_3$ is bis(*N*-alkylsalicylaldimine) complexes **3** (0.5–2.0 cal K^{-1} mol^{-1} (1 cal K^{-1} mol^{-1} =

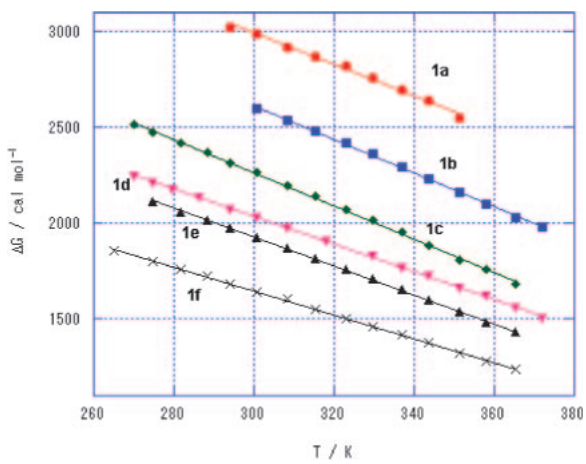

Figure 1. ΔG vs. T plots for **1a–1f** in toluene-d_8.

Table 2. Thermodynamic Data of Sp–Td Equilibria of **1a–1f** and **2a–2e** in Toluene-d_8 and $CDCl_3$

Complex	X or Y	Toluene-d_8		$CDCl_3$	
		ΔH/kcal mol^{-1} a)	ΔS/cal K^{-1} mol^{-1} a)	ΔH/kcal mol^{-1} a)	ΔS/cal K^{-1} mol^{-1} a)
1a	CF_3	5.44	8.1	3.72	5.0
1b	Cl	5.26	8.8	3.44	5.2
1c	H	4.87	8.7	3.16 (3.5)[b]	5.2 (4.8)[b]
1d	Me	4.19	7.5	2.72 (3.3)[b]	4.6 (4.7)[b]
1e	OMe	4.17	7.1	2.74	4.2
1f	NMe_2	3.52	6.2	2.37	4.1
2a	CF_3	5.61	11.4	5.07	10.4
2c	H	5.05	10.8	4.68	10.2
2d	Me	5.01	11.1	4.86	10.8
2e	OMe	4.84	10.6	4.97	11.0

a) 1 kcal mol^{-1} = 4.184 kJ mol^{-1}; 1 cal K^{-1} mol^{-1} = 4.184 J K^{-1} mol^{-1}. b) Ref. 3a.

Table 3. Thermodynamic Data of Sp–Td Equilibria of **1e** and **2c** in Various Solvents

Solvent	**1e**		**2c**	
	ΔH/kcal mol^{-1} a)	ΔS/cal K^{-1} mol^{-1} a)	ΔH/kcal mol^{-1} a)	ΔS/cal K^{-1} mol^{-1} a)
Toluene-d_8	4.17	7.1	5.05	10.8
C_6D_6	4.01	7.0	N.D.[b]	N.D.[b]
C_6D_5Cl	3.73	6.4	4.82	10.6
$CDCl_3$	2.74	4.2	4.68	10.2
$C_2D_2Cl_4$	2.22	3.3	4.27	9.1
CD_2Cl_2	2.41	3.7	4.11	9.3

a) 1 kcal mol^{-1} = 4.184 kJ mol^{-1}; 1 cal K^{-1} mol^{-1} = 4.184 J K^{-1} mol^{-1}. b) Not determined because of low solubility.

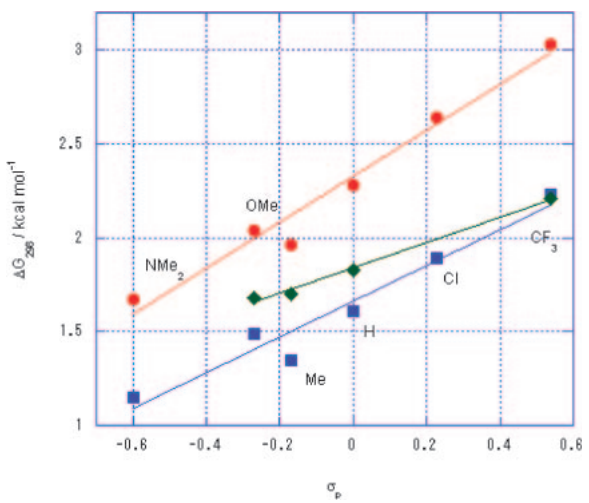

Figure 2. Plot of free energy change at 298 K vs. Hammett's σ_p value. Circle: **1a–1f** in toluene-d_8; square: **1a–1f** in $CDCl_3$; diamond: **2a–2e** in toluene-d_8.

4.184 J K^{-1} mol^{-1}))[4] < **1a–1f** < **2a–2e** ≤ nickel *N*,*N*′-diarylaminotroponeiminates **4** (9–13 cal K^{-1} mol^{-1}).[5] The entropy change is likely dependent on the molecular shape and number of aromatic rings: For complexes with more aromatic rings such as **2a–2e** and **4**, the ΔS values tend to increase.

For complexes **1a–1f**, the ΔH and ΔS values are smaller in $CDCl_3$ than in toluene-d_8. In order to investigate solvent effects on Sp–Td equilibria, we determined ΔH and ΔS for **1e** and **2c** in various non-coordinating solvents. As is seen in Table 3, ΔH tends to decrease in more polar solvents such as CD_2Cl_2 and 1,1,2,2-tetrachloroethane-d_2. Centrosymmetric Sp form has no net dipole moment, whereas the Td form has non-zero dipole moment (2.2 D estimated by DFT calculation) and hence is more stabilized in polar media. The ΔS values of **1e** are larger in aromatic solvents than in chlorohydrocarbon solvents. Since ΔS includes differences in spin multiplicity amounting to $R \ln 3$ (=2.18 cal K^{-1} mol^{-1}), other factors contribute only 2–3 cal K^{-1} mol^{-1} in the latter solvents. Similar solvent dependence was also observed for **3**.[4d] Because of the planar bis-chelate moiety, the Sp form is better solvated than the Td form especially in aromatic solvents. On the other hand, the Td form more effectively interacts with chlorohydrocarbon solvents through formation of C–H···O hydrogen bonds, since the oxygen atoms have more negative charge and are more exposed (vide infra, Figure 3 and Table 4). The ΔH and ΔS values for **2c** showed little solvent dependence. The oxygen atoms in the Td form of **2c** may be shielded from solvent molecules by the phenyl groups and/or the negative charge may be delocalized over the conjugated phenyl groups.

Interconversion Rates of Sp and Td Forms. For bis(phosphine)nickel dihalides, the interconversion rates between Sp and Td forms are 10^5 to 10^6 s^{-1} at 298 K. The ^{1}H NMR signals of Sp and Td forms are separately observed at low temperatures.[17] As an attempt to determine the conversion rates of the present complexes, the ^{1}H NMR spectrum of **1f** was recorded in CD_2Cl_2 at 196 K. The signal of β-protons was broadened but still coalesced, indicating that the interconversion process falls in a fast-exchange regime. At this temperature, the chemical shift difference will be 63400 Hz in a 400-MHz NMR

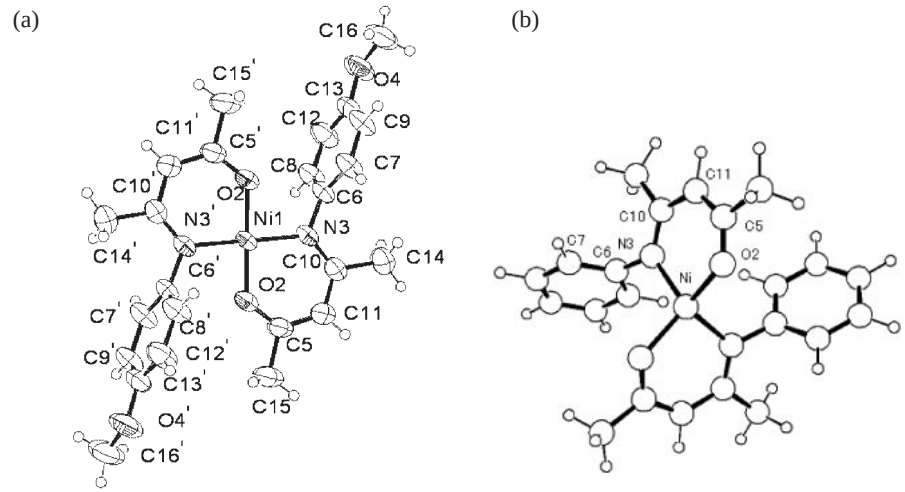

Figure 3. (a) ORTEP diagram of **1e** with thermal ellipsoids of 50% probability. (b) Molecular structure of Td form of **1c** optimized at UB3LYP/6-31G* level.

Table 4. NPA Atomic Charges and Spin Density

	Model **A** (X = F)		**1c** (X = H)		Model **B** (X = NH_2)	
	Sp	Td	Sp	Td	Sp	Td
Ni	1.034	1.370	1.038	1.372	1.033	1.368
N	−0.598	−0.680	−0.598	−0.676	−0.595	−0.673
O	−0.721	−0.782	−0.722	−0.783	−0.722	−0.784
Spin on Ni		1.602		1.603		1.601

spectrometer, assuming that Curie's law is obeyed. Qualitatively, the Sp–Td interconversion rate is much larger than 10^6 Hz even at 196 K. For bis(salicylaldimine) nickel complexes and nickel aminotroponeiminates, which were investigated by NMR at lower frequency (60–100 MHz), the interconversion processes were also fast in NMR timescale.[4,5] Thus, the Sp–Td conversions of bis-chelate complexes were faster than those of complexes with four unidentate ligands.

Origin of Substituent Effects on Sp–Td Equilibria. Eaton et al. reported for a series of nickel *N*,*N*′-bis(p-substituted phenylamino)troponeiminates **4** that the energy difference between Sp and Td forms is positively correlated with Taft's inductive substituent parameter, σ_I.[5] In the series of **1a–1f**, ΔG_{298} correlates with Hammett's substituent parameter, σ_p, rather than σ_I (Figure 2). This substituent effect is quite similar to that reported for bis(diarylmethylphosphine)nickel dihalides **5**.[6] In the phosphine complexes, the electronic effect was ascribed to the relative stabilization of the Sp form by electron-withdrawing substituents. According to the authors' interpretation, the energy level of 3p orbitals having π-character on the P atom is lowered with an increase in electron-withdrawing ability of the phosphine substituents and more strongly interacts with the Ni d_{xy} orbital. Such interaction stabilizes the occupied d_{xy} orbital and destabilizes the unoccupied $d_{x^2-y^2}$ orbital. This substituent effect on the ligand field strength is opposite to that observed for **1a–1f** (Table 1).

The electronic substituent effect on the relative stability of Sp and Td forms might be accounted for in terms of the energy level of MOs and/or charge or spin delocalization into the ligands. We carried out structure optimization and population analyses for unsubstituted complex **1c** (X = H), model **A** (X = F) having electron-withdrawing substituents, and model **B** (X = NH_2) having electron-releasing substituents by DFT calculation at B3LYP/6-31G* level to compare the electronic properties among the three. The molecular geometry of the Sp form can be obtained from the X-ray structure analysis of **1e** (Figure 3a), which was used as the initial structure for optimization of the Sp form of **1c**. As is seen in Table 5, the calculated bond distances and angles fairly well reproduce the observed values. The chelate ring is essentially planar, and the phenyl groups are almost perpendicular to the chelate plane. The structure is quite similar to that reported for the same type of nickel complex with different *N*-aryl groups.[18] The optimized structure in Td form of **1c** (X = H) is shown in Figure 3b. The phenyl groups are also largely twisted from the chelate plane. The bite angle (94.7°) of O–Ni–N is smaller than N–Ni–N and O–Ni–O angles, indicating flattering distortion from regular tetrahedral coordination. Similar distorted tetrahedral coordination is reported for a bis(salicylaldimine)-nickel complex with bulky substituents on the N atoms.[19] The Ni–N and Ni–O distances in Td form are longer than the corresponding distances in Sp form, suggesting that coordination bonding is weaker in Td form than in Sp form. Structures of Sp

Table 5. Selected Geometrical Parameters Observed for **1e** and Calculated for **1c**[a)]

	Sp obsd (**1e**)	Sp calcd (**1c**)	Td calcd (**1c**)
Ni1–N3/Å	1.921(1)	1.925	1.955
Ni1–O2/Å	1.820(1)	1.818	1.911
C5–O2/Å	1.282(2)	1.284	1.283
C10–N3/Å	1.317(3)	1.332	1.331
C11–C5/Å	1.359(3)	1.385	1.397
C11–C10/Å	1.409(3)	1.412	1.415
O2–Ni1–N3/°	92.83(6)	92.9	94.7
N3–Ni–N3′/°	180	180	121.2
O2–Ni–O2′/°	180	180	134.4
C10–N3–C6–C7/°	82.4	89.7	69.3

a) The numbering scheme is shown in Figure 3a.

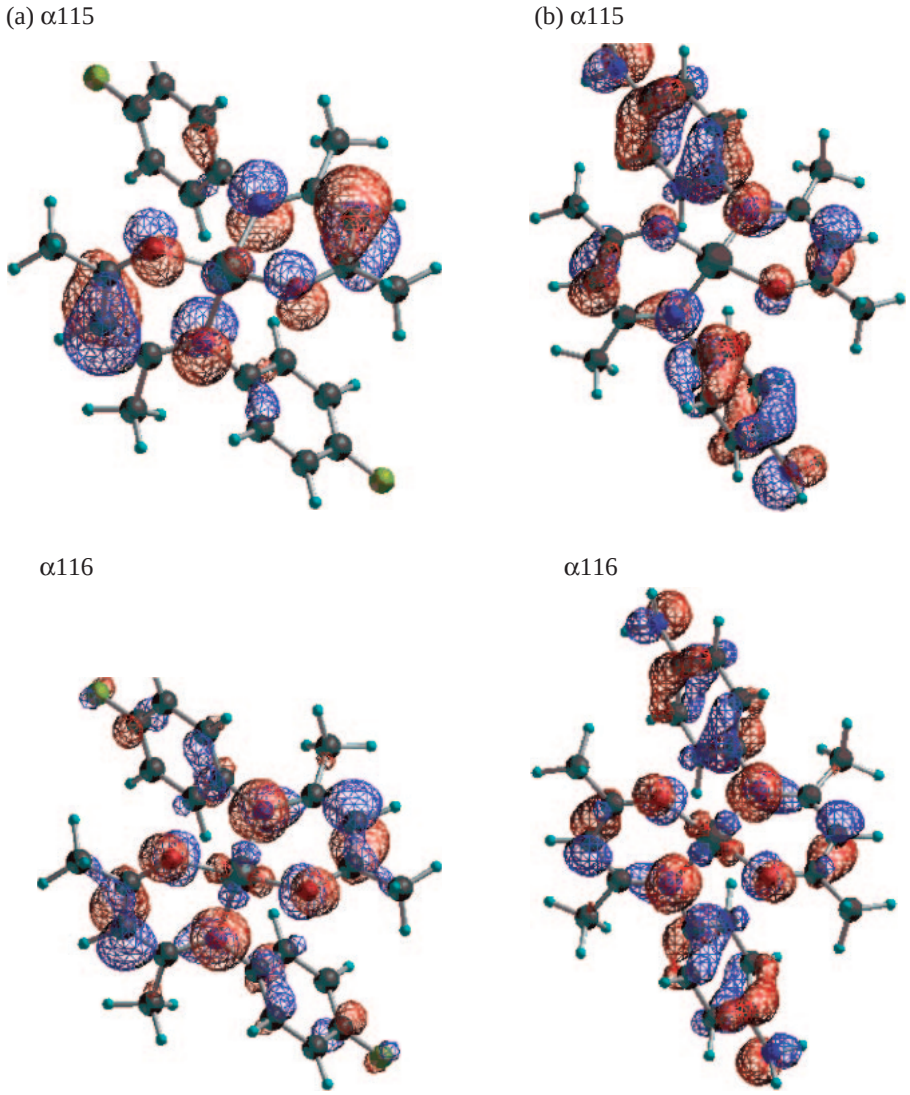

Figure 4. Visualized SOMOs for (a) model **A** (X = F) and model **B** (X = NH_2).

and Td forms of either model are closely similar to those of **1c**.

The energy differences of Td form versus Sp form, ΔE, were obtained by single-point calculation with slightly larger basis sets (see Experimental). The ΔE values (difference in zero-point energy is not included) are -0.75, -1.13, and $-1.44\,\mathrm{kcal\,mol^{-1}}$ ($1\,\mathrm{kcal\,mol^{-1}} = 4.184\,\mathrm{kJ\,mol^{-1}}$) for model **A**, **1c**, and model **B**, respectively. Spin-restricted SCF calculations of Td form were also performed for "fair" comparison of the energy with closed shell Sp form. In this case, the ΔE values are $+0.69$, $+0.31$, and $0.00\,\mathrm{kcal\,mol^{-1}}$. Thus, Sp and Td forms are substantially the same in thermodynamic stability. Electron-donating groups somewhat stabilize the Td form relative to Sp form. These features, at least qualitatively, agree with the experimental results.

The character of several MOs will be discussed. In the Sp form of **1c**, the HOMO consists of the β-ketoiminate O–C–C–C–N π-system (70%) and Ni d orbitals (22%). The energy of the HOMO in model **A** decreases by 0.16 eV while that in model **B** increases by 0.18 eV as compared with that in **1c**. The character of the HOMO is, however, essentially unaffected by the substituents. In model **B**, HOMO$-$1 and HOMO$-$2 are localized on the $-C_6H_4NH_2$ groups, HOMO$-$3 is on the β-ketoiminate, and HOMO$-$4 is essentially the Ni d_{z^2} orbital. In **1c** and model **A**, HOMO$-$1 is localized on the β-ketoiminate π-system and HOMO$-$2 is essentially the Ni d_{z^2} orbital. In any case, the LUMO has a significant coefficient of Ni $d_{x^2-y^2}$ orbital. Although the electron-rich aryl groups somewhat affect the frontier orbitals, the substituent effect on the electronic structure is small. In Td form, the molecule has two SOMOs (115th and 116th MOs for models **A** and **B**; 107th and 108th MOs for **1c**). In model **A** (Figure 4a) and **1c**, electron density is mainly over the β-ketoiminate moieties and some on Ni. On the other hand, the corresponding MOs in model **B** have large contribution from the $C_6H_4NH_2$ groups (Figure 4b). The phenyl π-orbitals in model **B** have increased energy due to the electron-donating NH_2 groups and interact with the β-ketoiminate π-orbitals more strongly than in the cases of **1c** and model **A**. Such interaction, however, rises in energy these occupied orbitals and hence cannot account for the relative stabilization of the Td form by electron-donating substituents. The corresponding unoccupied β orbitals mainly consist of the Ni d orbitals and the β-ketoiminate π-orbitals in

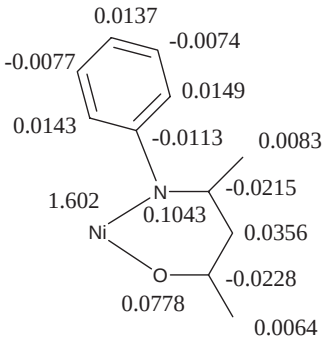

Figure 5. Spin densities of non-H atoms in **1c**.

model **A**, **1c**, and model **B**, and no significant difference is observed among the three.

Holm et al. studied spin delocalization onto the ligands from the observed ^{1}H hyperfine coupling constants and the spin densities calculated for the O=C–C=C–N• π-radical by Hückel MO methods.[3,4] They estimated that the fractional spin delocalization was ca. 1/20 for each ligand and proposed that such spin transfer should be induced through dπ–pπ orbital interaction.[3a] The spin densities in the Td form of **1c** obtained by DFT calculation are illustrated in Figure 5. The nickel atom bears 1.6 α-spins and the remaining part is distributed over the ligands. Among the C atoms, the β-carbon has the largest spin polarization, which is consistent with the fact that the β-proton shows the largest hyperfine interaction. A number of MOs (for example, α115 orbital in Figure 4a) are composed of both the β-ketoiminate pπ orbitals and Ni dπ orbitals. These features indicate that dπ–pπ bonding interaction has some contribution to the metal–ligand bonding. Significant spin polarization is also induced in the phenyl groups, especially at o- and p-positions. This trend is consistent with the observation that the phenyl protons exhibited relatively large contact shifts (not shown). The spin distribution is almost the same in models **A** and **B**, indicating that the substituent effect on the spin delocalization is negligibly small.

Although atomic charges cannot unequivocally be determined from ab initio or DFT calculations, NPA (natural population analysis[20]) atomic charges may provide some information on metal–ligand bonding. As is seen in Table 4, more electrons are transferred to the metal from the ligand in Sp form than in Td form. The oxygen atoms have more negative charge in Td form than in Sp form. The more negative charge is more favorable to form a hydrogen bond with solvent such as chloroform. As for the substituent effect on the atomic charges, the N atoms in model **B** bear less negative charge that those in **1c** or model **A** while the Ni atom in model **B** is less positive than that in the latter. The electron-donating substituent may help the N atoms donate more electrons to the Ni atom. The effect is; however, small and such tendency is also seen in Sp form.

In conclusion, the energy differences between Sp and Td forms of **1a**–**1f** and **2a**–**2e** are small, and equilibria are rapidly established in solution. The equilibrium constants vary with the electronic nature of substituents, but the origin of the effect seems to be a quite subtle balance among several factors that can influence the electronic structure. In **1a**–**1f**, the enthalpy and entropy changes depend on the properties of solvent. This observation can be explained in terms of dipole–dipole and hydrogen-bonding interaction with the solvent molecules.

We thank Professor Akihiko Yamagishi and Dr. Hisako Sato, Ochanomizu University, for their continuous encouragement and discussion. We are greatly indebted to Professor Yuichi Masuda, Ochanomizu University, for his fruitful discussion on NMR data analyses. Thanks are also due to Professor Keiko Takano, Ochanomizu University, for her help with DFT calculation. This work was financially supported by NEDO.

Supporting Information

^{1}H NMR (400 MHz) spectra at ambient temperature of **1b**–**1f**, **2c**, and **2d** and the temperature dependence of chemical shift of β-protons of **1a**–**1f** in $CDCl_3$. This material is available free of charge of the Web at: http://www.csj.jp/journals/bcsj/.

References

1 K. Sone, Y. Fukuda, *Inorganic Thermochromism, Inorganic Chemistry Concept*, Springer, Heidelberg, **1987**, Vol. 10.

2 a) M. Schumann, A. von Holtum, K. J. Wannowius, H. Elias, *Inorg. Chem.* **1982**, *21*, 606. b) M. Schumann, H. Elias, *Inorg. Chem.* **1985**, *24*, 3187.

3 a) G. W. Everett, Jr., R. H. Holm, *J. Am. Chem. Soc.* **1965**, *87*, 2117. b) G. W. Everett, Jr., R. H. Holm, *Inorg. Chem.* **1968**, *7*, 776.

4 a) L. Sacconi, P. Paoletti, M. Ciampolini, *J. Am. Chem. Soc.* **1963**, *85*, 411. b) R. H. Holm, A. Chakravorty, G. O. Dudek, *J. Am. Chem. Soc.* **1964**, *86*, 379. c) R. Knoch, H. Elias, H. Paulus, *Inorg. Chem.* **1995**, *34*, 4032. d) R. H. Holm, A. Chakravorty, G. O. Durek, *J. Am. Chem. Soc.* **1964**, *86*, 379.

5 D. R. Eaton, W. D. Phillips, D. J. Caldwell, *J. Am. Chem. Soc.* **1963**, *85*, 397.

6 L. H. Pignolet, W. D. Horrocks, Jr., R. H. Holm, *J. Am. Chem. Soc.* **1970**, *92*, 1855.

7 C. J. Valduga, A. Squizani, H. S. Braibante, M. E. F. Braibante, *Synthesis* **1998**, 1019.

8 R. H. Holm, F. Röhrscheid, G. W. Everett, Jr., I. L. Madden, J. M. Grow, L. J. Todd, *Inorg. Synth.* **1968**, *11*, 72.

9 N. S. Gill, R. S. Nyholm, *J. Chem. Soc.* **1959**, 3997.

10 **1b**: S. Yamada, H. Nishikawa, E. Yoshida, *Bull. Chem. Soc. Jpn.* **1966**, *39*, 994; **1e**: N. Raman, V. Muthuraj, S. Ravichandran, *J. Indian Chem. Soc.* **2005**, *82*, 443; **1f**: S. K. Agarwal, R. C. Saxena, *J. Indian Chem. Soc.* **1979**, *56*, 925; **1c**, **1d**, and **2c**: G. W. Everett, Jr., R. H. Holm, *J. Am. Chem. Soc.* **1965**, *87*, 2117; **2d**: W. K. Musker, H. S. Hussain, *Inorg. Chem.* **1966**, *5*, 1416.

11 a) A. L. Van Geet, *Anal. Chem.* **1970**, *42*, 679. b) D. S. Raiford, C. L. Fisk, E. D. Becker, *Anal. Chem.* **1979**, *51*, 2050.

12 A. Chakravorty, R. H. Holm, *J. Am. Chem. Soc.* **1964**, *86*, 3999.

13 D. H. Gerlach, R. H. Holm, *J. Am. Chem. Soc.* **1969**, *91*, 3457.

14 A. Altomare, G. Cascarano, C. Giacovazzo, A. Guagliardi, M. C. Burla, G. Polidori, M. Camalli, *J. Appl. Crystallogr.* **1994**, *27*, 435.

15 G. M. Sheldrick, *SHELXL97, Program of the Refinement of Crystal Structures*, University of Göttingen, Germany, **1997**.

16 M. J. Frisch, G. W. Trucks, H. B. Schlegel, G. E. Scuseria, M. A. Robb, J. R. Cheeseman, J. A. Montgomery, Jr., T. Vreven, K. N. Kudin, J. C. Burant, J. M. Millam, S. S. Iyengar, J. Tomasi, V. Barone, B. Mennucci, M. Cossi, G. Scalmani, N. Rega, G. A. Petersson, H. Nakatsuji, M. Hada, M. Ehara, K. Toyota, R. Fukuda, J. Hasegawa, M. Ishida, T. Nakajima, Y. Honda, O. Kitao, H. Nakai, M. Klene, X. Li, J. E. Knox, H. P. Hratchian, J. B. Cross, C. Adamo, J. Jaramillo, R. Gomperts, R. E. Stratmann, O. Yazyev, A. J. Austin, R. Cammi, C. Pomelli, J. W. Ochterski, P. Y. Ayala, K. Morokuma, G. A. Voth, P. Salvador, J. J. Dannenberg, V. G. Zakrzewski, S. Dapprich, A. D. Daniels, M. C. Strain, O. Farkas, D. K. Malick, A. D. Rabuck, K. Raghavachari, J. B. Foresman, J. V. Ortiz, Q. Cui, A. G. Baboul, S. Clifford, J. Cioslowski, B. B. Stefanov, G. Liu, A. Liashenko, P. Piskorz, I. Komaromi, R. L. Martin, D. J. Fox, T. Keith, M. A. Al-Laham, C. Y. Peng, A. Nanayakkara, M. Challacombe, P. M. W. Gill, B. Johnson, W. Chen, M. W. Wong, C. Gonzalez, J. A. Pople, *Gaussian 03, Rev. D01*, Gaussian, Inc., Pittsburgh PA, **2003**.

17 a) G. N. La Mar, E. O. Sherman, *J. Am. Chem. Soc.* **1970**, *92*, 2691. b) L. H. Pignolet, W. D. Horrocks, Jr., *J. Am. Chem. Soc.* **1968**, *90*, 922. c) L. Que, Jr., L. H. Pignolet, *Inorg. Chem.* **1973**, *12*, 156.

18 X. He, Y. Yao, X. Luo, J. Zhang, Y. Liu, L. Zhang, Q. Wu, *Organometallics* **2003**, *22*, 4952.

19 T. Akitsu, Y. Einaga, *Polyhedron* **2005**, *24*, 1869.

20 A. E. Reed, L. A. Curtiss, F. Weinhold, *Chem. Rev.* **1988**, *88*, 899.